

# Plasma oxidation of Cu–Al alloy

JUN TAKADA

*Department of Applied Chemistry, Okayama University, Okayama 700, Japan*

HIDEYUKI KUWAHARA

*Research Institute for Applied Science, Kyoto 606, Japan*

YUUJI MANABE, MITSUO KIMURA, KENJI YANAGIHARA

*Research Center, Japan Synthetic Rubber Co. Ltd, Tsukuba 305, Japan*

Selective oxidation of Cu–1.0 wt % Al alloy was found to be achieved by using microwave plasma at 1073 K in a mixed gas of 10 % O<sub>2</sub> and 90 % N<sub>2</sub> at a total pressure of 2 torr (~266.644 Pa). The selective oxidation was confirmed by electron diffraction analysis of aluminium oxide particles, microstructural observations and hardness measurements of the internal oxidation layer. Electrical conductivity and the thermal expansion coefficient of the oxidized specimens were measured. The morphology and distribution of the aluminium oxide particles formed in the oxidized alloy is also discussed.

## 1. Introduction

Low-temperature plasma has been used for diamond synthesis, rearrangement of the molecular structure of polymers, and modification of solid surfaces, such as in the coating of thin films of carbide, nitride, boride or oxide. As an example of the surface modification of metals, plasma nitriding forms nitrides of the metals on a specimen surface to provide many practical merits: increased strength, shorter periods of heat treatment, lower heat-treatment temperatures [1–3]. Little information is, however, available on the plasma oxidation of metals.

The usual oxidation of alloys using an equilibrium reaction of gas and metal has been studied by many investigators [4–10]. In alloys containing a solute element less noble than a solvent metal, the formation of two different oxidation layers is well known: an external oxidation layer consisting of the oxides of both the solvent and the solute elements, and an internal oxidation layer with small oxide particles of the solute element dispersed throughout the matrix metal [4, 7]. Under a relatively low oxygen partial pressure, only the internal oxidation layer is formed [6–10]. The layer gives strength, especially at elevated temperatures, to the alloy. Electrical conductivity is also often higher in the internally oxidized alloys than in those before oxidation [10]. Although alloys can also be hardened by addition of one or more solute elements (solution hardening), electrical conductivity is lower in most of the solution-hardened alloys than in the base metal [7, 10].

Although the plasma oxidation of alloys is thus of great interest from the practical and basic points of view, no study of plasma oxidation has been reported previously. It is, therefore, important to clarify

whether or not solid alloys can be oxidized using plasma. The aim of this study was to look at the possibility of oxidation of alloys using low-temperature plasma. If plasma oxidation of alloys is possible, it will be necessary to study the plasma oxidation behaviour, microstructure and some physical properties, such as hardness and electrical conductivity, and compare them with those for alloys oxidized in gas without plasma. For these purposes, we chose a Cu–1.0 wt % Al alloy as the sample, because much information on the oxidation behaviour in gas and the physical properties of copper alloys is known [4–8].

## 2. Experimental procedure

A Cu–1.0 wt % Al alloy, whose chemical composition is shown in Table I, was prepared by vacuum melting. The alloy was cold-rolled and cut to a plate specimen of 5 × 50 × 0.2 mm<sup>3</sup>. Before oxidation, these specimens were mechanically polished and annealed at 1073 K for 7.2 ks in vacuum to remove strain, giving an average grain size of about 0.10 mm.

Fig. 1 shows a block diagram of the plasma oxidation equipment used. Oxidation was conducted at 1073 K for various periods from 1.8–36 ks using a microwave plasma with a frequency of 2.45 GHz and an input power of 800 W in a mixed gas of 10 % O<sub>2</sub> and 90 % N<sub>2</sub> with a total gas pressure of 2.0 torr (~266.644 Pa). Oxidation temperature was controlled by both plasma and an additional heating device (H) as shown in Fig. 1.

The specimens oxidized using plasma were cut into halves and each cross-section was mechanically polished. The appearance and the thickness of the oxidation layer were then examined using an optical

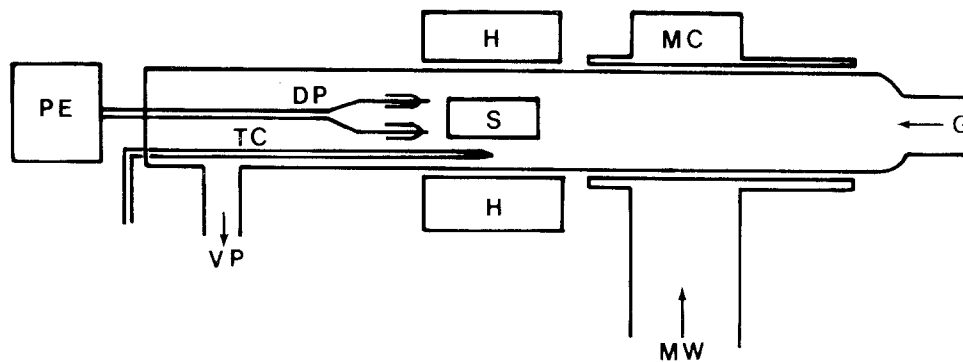


Figure 1 Block diagram of the plasma-oxidation equipment used. S, the specimen; H, the additional heater; MW, the microwave; MC, the microwave cavity; G, the flow gas; VP, the vacuum pump; TC, the thermocouple; DP, the double probe; PE, the probe equipment.

TABLE I Chemical composition of the alloy used (wt %)

Al	S	C	O
0.99	0.001	0.01	0.001

microscope equipped with a micrometer. Microhardness measurements were conducted on each cross-section under a load of 10 g using a Vickers microhardness tester.

Electrical resistivity measurements were made at room temperature by the usual double-probe method. The thermal expansion coefficient of the oxidized alloy was also examined using a thermomechanical analyser (Rigaku TMA-8140).

Electron microscopic observation of extraction replicas was carried out in order to determine the structure, the morphology and the distribution of the aluminium oxide formed in the alloy by plasma oxidation. After being mechanically polished, the cross-section of the specimen was electropolished in a solution of 70% orthophosphoric acid and 30% water. It was etched lightly and thoroughly washed. An extraction carbon replica was taken from the cross-section, bringing oxide particles with it. The replica was mounted in an electron microscope and photographed.

### 3. Results and discussion

Fig. 2 shows the typical microstructure of the alloy plasma oxidized at 1073 K for 1.8 ks. S indicates the specimen surface and F the oxidation front, i.e. the interface between the oxidized and the unoxidized regions. The oxidation layer, of which the front advances parallel to the specimen surface, can be clearly observed. In the present alloy oxidized using plasma, the thickness of the oxidation layer was 78  $\mu\text{m}$ .

Fig. 3 shows the hardness profile on a cross-section of the same sample as shown in Fig. 2. Two regions are clearly distinguishable; the oxidized layer and the unoxidized region. The thickness of the oxidized layer, which is about 70  $\mu\text{m}$  (Fig. 3) is in agreement with that obtained from the microstructural observation in Fig. 2. The hardness,  $H_v = 178$ , in the oxidized layer is higher than that ( $H_v = 74$ ) of the unoxidized region,

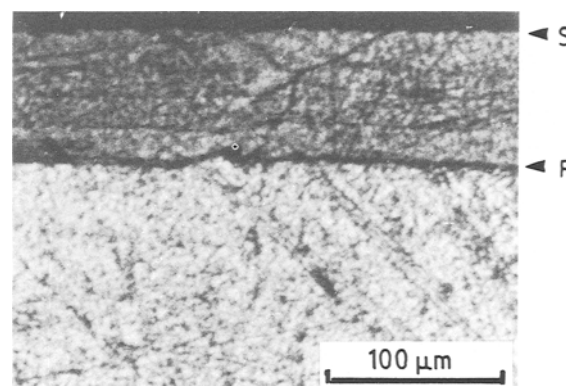


Figure 2 The typical microstructure of Cu-1.0 wt % alloy plasma-oxidized at 1073 K for 1.8 ks. S and F represent the specimen surface and the oxidation front, respectively.

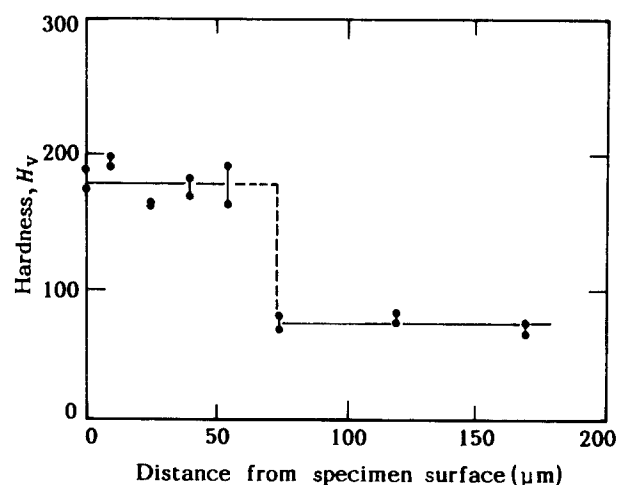


Figure 3 Hardness profile for the specimen shown in Fig. 2.

and remains almost constant throughout the layer. Furthermore, the hardness in the oxidized layer is approximately 4.5 times as high as that in the matrix metal, copper. The oxidized layer is a so-called internal oxidation layer where the solute element, aluminium, is selectively oxidized to form precipitates of  $\text{Al}_2\text{O}_3$  [4, 5, 7, 8]. The increase in hardness is due to the dispersion of small  $\text{Al}_2\text{O}_3$  particles throughout the copper matrix. Thus, the plasma oxidation of Cu-Al alloy is markedly effective in strengthening copper alloys.

The thickness value of the layer in the plasma-oxidized specimen as shown in Figs 2 and 3 is much larger than that (30  $\mu\text{m}$ ) in the specimen oxidized at 1073 K for 3.6 ks using an equilibrium reaction of copper and  $\text{Cu}_2\text{O}$  (the Rhines method), in which  $\text{Cu}_2\text{O}$  powders surrounding the Cu–Al alloy supply oxygen to the copper by a dissociation reaction in a thermal equilibrium at a particular temperature. The acceleration of the internal oxidation rate in plasma oxidation may result from large amount of dissolved oxygen in the alloy at the specimen surface. It may be because oxygen supplied to the specimen surface is as its active ions and/or as radicals in the plasma. The electron temperature,  $T_e$ , in the plasma is one of the important factors which control the plasma oxidation. A detailed discussion of  $T_e$  in the oxidation of the present alloy using a low-temperature plasma will be reported elsewhere [11].

The electrical conductivity of the alloy plasma oxidized at 1073 K was 76% IACS, which was much higher than that (38% IACS) of the unoxidized Cu–1.0 wt % Al alloy. It is also noteworthy that the electrical conductivity in the present alloy is much higher in comparison with that for electrical contact materials, such as Cu–4.2 Sn–0.2 P, Cu–5.0 Zn and Cu–1.5 Ni–0.5 Be alloys. For the latter three alloys, the values of electrical conductivity are 20, 56 and 48% IACS, respectively, at 293 K [12]. Thermal expansion coefficient of the same sample as shown in Fig. 2 was  $1.51 \times 10^{-5} \text{ K}^{-1}$ , a little lower than that of pure copper,  $1.81 \times 10^{-5} \text{ K}^{-1}$ .

Fig. 4 shows typical electron micrographs of an extraction replica for the Cu–1.0 wt % Al alloy plasma oxidized at 1073 K for 7.2 ks. Fig. 4a and b show the microstructure and an electron diffraction pattern, respectively. The uniform and dense dispersion of

small aluminium oxide particles with hexagonal or nearly circular shapes can easily be seen. Similar results have been reported in copper alloy single crystals with 0.051–0.198 wt % Al oxidized in the temperature range 1173–1273 K by the Rhines method [8]. The diffraction pattern in Fig. 4b reveals that the aluminium oxide formed by plasma oxidation is  $\gamma\text{-Al}_2\text{O}_3$ , in agreement with that formed by the Rhines pack method [5].

It can be concluded from Figs 2 and 4 that the Cu–Al alloy can be internally oxidized using low-temperature plasma of oxygen and the oxidation rate is accelerated. It can be emphasized that an external oxidation layer of copper oxides is negligibly thin, resulting in the very smooth specimen surface as shown in Fig. 2. This result is in contrast to the rough surface obtained due to the irregular formation of copper in alloys oxidized by the Rhines method.

The particle diameter and the number of the oxide particles were carefully measured from Fig. 4a. Fig. 5a shows a distribution function,  $F(x)$ , of oxide particle diameter,  $x$ , indicating that the particle distribution does not obey to a Gaussian distribution. A cumulative distribution function of the particle diameter,  $P(x)$ , namely the number of particles with diameter less than  $x$ , can be calculated from the information on the particle diameter in the distribution function.  $P(x)$ , as obtained, was plotted against  $x$  on log-normal probability paper as shown in Fig. 5b;  $P(x)$  approximates to a straight line in the graph. Thus, the distribution of the particle diameter in the plasma-oxidized alloy was found approximately to be in accord with a log-normal one. Similar results have been reported in Cu–Al and Cu–Si alloys oxidized by the Rhines method [5, 8]. The geometric mean of particle diameter,  $d$ , in the present alloy is 42 nm as shown in

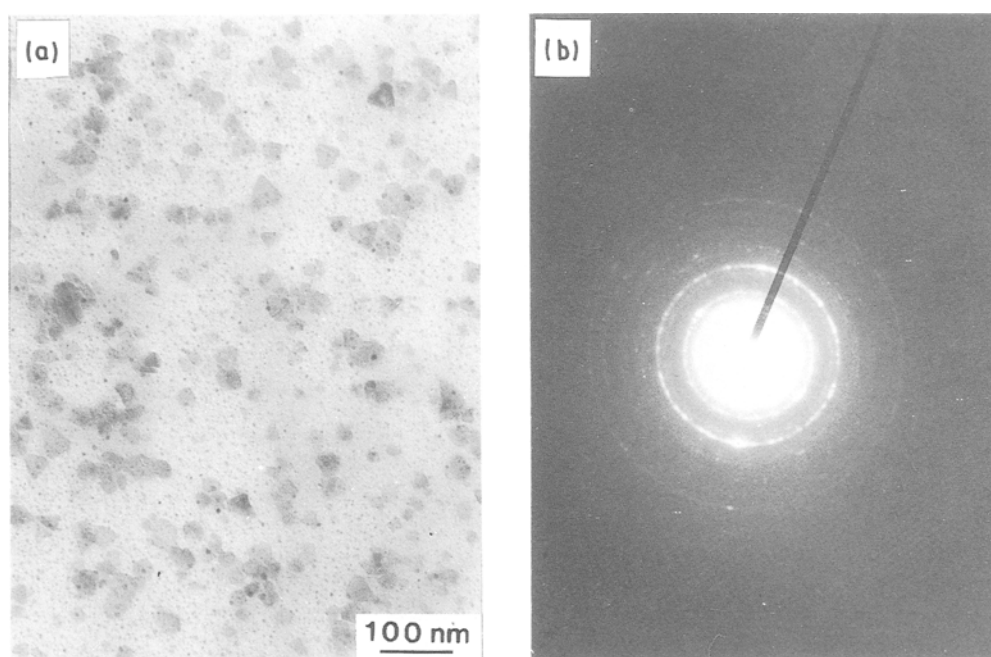


Figure 4 (a) Electron micrograph of an extraction replica, and (b) electron diffraction pattern of the aluminium oxide in Cu–1.0 wt % Al alloy plasma-oxidized at 1073 K for 7.2 ks.

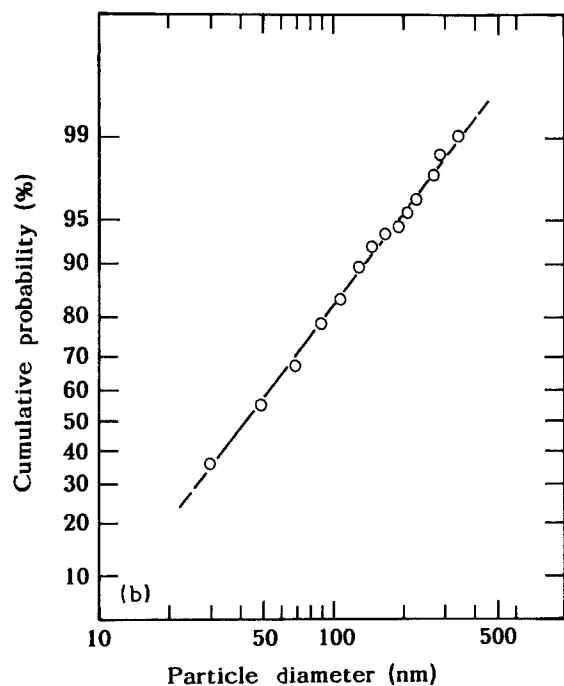
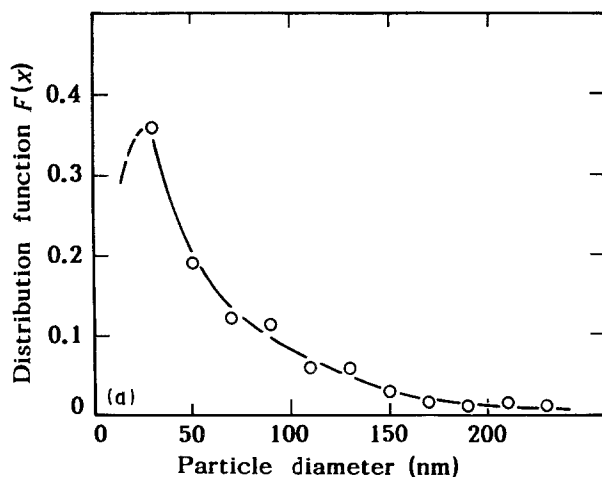


Figure 5 (a) Distribution function, and (b) cumulative distribution function of particle diameter of the aluminium oxide formed in the alloy shown in Fig. 4.

Fig. 5b. Furthermore, the centre-to-centre particle spacing,  $S$ , was calculated to be 290 nm using the number of the oxide particles per unit area.

Using the values of  $d$  and  $S$  obtained, the contribution of the dispersed particles to the strength of the alloy can be estimated. The increase in critical shear stress in the dispersion-strengthened alloys is determined by the Orowan stress [13],  $\tau_p$

$$\tau_p = \frac{0.81 Gb}{2\pi(1-\nu)^{1/2} \lambda} \ln\left(\frac{b}{r_0}\right) \quad (1)$$

where  $G$  is the shear modulus,  $b$  the Burgers vector,  $\nu$  Poisson's ratio,  $r_0$  the inner cut-off radius of the dislocation energy calculation and  $\lambda (= S - d)$  the particle spacing.  $\tau_p$  in the present alloy was estimated to be  $3.00 \text{ kg mm}^{-2}$  (29.4 MPa) using  $S$  and  $d$  values obtained,  $G = 4220 \text{ kg mm}^{-2}$  (41.4 GPa),

$\nu = 1/3$  and  $r_0 = 2b$  [8]. Furthermore, the increase in tensile yield stress,  $\sigma_p$ , was calculated to be  $27.6 \text{ kg mm}^{-2}$  (271 MPa) on the basis of Taylor's relationship between shear and tensile yield stresses [14]. Unfortunately, it is impossible to compare  $\sigma_p$  with an increase in hardness,  $\Delta H_v$ , due to the particle dispersion shown in Fig. 4, because the relationship between yield stress and hardness is not clear in this alloy at present. Further study is now in progress.

#### 4. Conclusions

The oxidation using a low-temperature plasma of Cu-1.0 wt % Al alloy was conducted at 1073 K in a gaseous mixture of 10%  $\text{O}_2$  and 90%  $\text{N}_2$ . Microstructural observations, measurements of microhardness and electrical conductivity were conducted. Aluminium oxide particles formed in the oxidized alloy were identified and their shape and distribution were determined using electron microscopy. The main results were as follows.

1. The oxidation layer with a front advancing parallel to the specimen surface was distinguished from the unoxidized region by both microstructural observations and hardness measurements. The thickness of the oxidized layer was approximately  $78 \mu\text{m}$  for the alloy oxidized at 1073 K for 1.8 ks. High hardness of  $H_v = 178$  remains constant throughout the oxidized layer.

2. The aluminium oxide formed in the present alloy was found to be  $\gamma\text{-Al}_2\text{O}_3$ . The  $\text{Al}_2\text{O}_3$  particle diameter distribution is log-normal, not Gaussian. The average diameter and spacing of the oxide particles were 42 and 290 nm, respectively.

3. Plasma oxidation was therefore found to be achieved using a low-temperature plasma of an  $\text{O}_2\text{-N}_2$  gas mixture in the present Cu-Al alloy.

4. The thickness of the layer is much larger for plasma oxidation using a low-temperature plasma than for oxidation under equilibrium oxygen pressure of the dissociation of  $\text{Cu}_2\text{O}$  into copper (the Rhines method).

5. The electrical conductivity and thermal expansion coefficient of the oxidized alloy were 76% IACS and  $1.51 \times 10^{-5} \text{ K}^{-1}$ , respectively.

#### References

1. H. KNUPELL, K. BROTZMANN and F. EBERHARD, *Stahl und Eisen* **78** (1958) 1871.
2. J. TAKADA, Y. OHIZUMI, H. MIYAMURA, H. KUWAHARA, S. KIKUCHI and I. TAMURA, *J. Mater. Sci.* **21** (1986) 2493.
3. H. KUWAHARA, J. TAKADA and I. TAMURA, in "Proceedings of the 8th International Symposium on Plasma Chemistry", Tokyo, September 1987, edited by K. Akashi (International Union of Pure and Applied Chemistry, Eindhoven, 1987) p. 1709.
4. F. N. RHINES, W. A. JOHNSON and W. A. ANDERSON, *Trans. Met. Soc. AIME* **147** (1942) 205.
5. M. F. ASHBY and G. C. SMITH, *Phil. Mag.* **5** (1960) 298.
6. J. E. VERFURTH and R. A. RAPP, *Trans. Met. Soc. AIME* **230** (1964) 1310.

7. J. H. SWISHER, in "Oxidation of Metals and Alloys" (ASM, Metals Park, Ohio, 1971) p. 235.
8. J. TAKADA, S. MIYAWAKI, K. KAMATA and M. ADACHI, *Trans. Jpn. Inst. Metals* **25** (1984) 784.
9. J. TAKADA, S. YAMAMOTO, S. KIKUCHI and M. ADACHI, *Met. Trans.* **17A** (1986) 221.
10. N. YOSHIDA, Y. TOMII, J. TAKADA, S. KIKUCHI and M. KOIWA, *Trans. Jpn. Inst. Metals* **29** (1988) 693.
11. K. YANAGIHARA, M. KIMURA, Y. MANABE, H. KUWAHARA and J. TAKADA, in "Proceedings of 5th Symposium on Plasma Processing", Yokohama, January 1988, edited by T. Makabe (Japan Society of Applied Physics) p. 167.
12. "Metals Handbook", 9th Edn, Vol. 2 (ASM, Metals Park, OH, 1979) pp. 316, 354, 438.
13. P. B. HIRSCH and F. J. HUMPHREYS, in "Physics of Strength and Plasticity" (MIT Press, 1969) p. 189.
14. G. I. TAYLOR, *J. Inst. Metals* **62** (1938) 307.

*Received 3 August 1990  
and accepted 12 February 1991*